Published in final edited form as:
In Vivo. 2010 ; 24(1): 1–8.

Effectiveness of Combined Modality Radiotherapy of Orthotopic Human Squamous Cell Carcinomas in Nu/Nu Mice Using Cetuximab, Tirapazamine and MnSOD-Plasmid Liposome Gene Therapy

MICHAEL W. EPPERLY[1], **STEPHEN Y. LAI**[2], **ANTHONY J. KANAI**[3], **NEAL MASON**[4], **BRIAN LOPRESI**[4], **TRACEY DIXON**[1], **DARCY FRANICOLA**[1], **YUNYUN NIU**[1], **WILLIAM R. WILSON**[5], and **JOEL S. GREENBERGER**[1]

[1] Department of Radiation Oncology, University of Pittsburgh Cancer Institute, Pittsburgh, PA, U.S.A
[2] Department of Otolaryngology, University of Pittsburgh Cancer Institute, Pittsburgh, PA, U.S.A [3] Department of Medicine, University of Pittsburgh Cancer Institute, Pittsburgh, PA, U.S.A [4] Department of Diagnostic Radiology, University of Pittsburgh Cancer Institute, Pittsburgh, PA, U.S.A
[5] Auckland Cancer Research Center, University of Auckland, Auckland, New Zealand

Abstract

Hypoxic regions limit the radiocontrollability of head and neck carcinomas. Whether or not combinations of plasmid/liposome mediated overexpression of normal tissue protective manganese superoxide dismutase (MnSOD), cetuximab (C225), and the hypoxic cytotoxin tirapazamine (TPZ) enhanced radiotherapeutic effects was tested in a CAL-33 orthotopic mouse cheek tumor model. The tumor volume continued to increase in the control (untreated) mice, with a ninefold increase by 10 days when the tumors exceeded 2 cm^3. The mice receiving 14 Gy only showed reduced tumor growth to 3.1±0.1 fold at day 10. The mice receiving MnSOD-PL, C225, TPZ plus 14 Gy had the best outcome with 0.7±0.1 fold increase in tumor volume by 10 days ($p=0.015$) compared to irradiation only. The addition of MnSOD-PL, TPZ, and C225 to irradiation optimized the therapeutic ratio for the local control of hypoxic region-containing CAL-33 orthotopic tumors.

Keywords

Orthotopic tumors; MnSOD-PL; cetuximab; tirapazamine

Combined modality chemoradiotherapy of squamous cell carcinomas of the head and neck is complicated due to normal tissue toxicity (1–5). Despite the availability of sophisticated intensity-modulated radiotherapy treatment planning techniques and frameless stereotactic radiotherapy modalities, normal tissue toxicity remains a dose-limiting problem in therapeutic programs (3–5). Improving the therapeutic ratio (ratio of tumor cell killing to normal tissue toxicity) remains a major challenge in clinical radiotherapy. In attempts to improve the quality of life and overall survival of head and neck cancer patients, new chemotherapeutic agents and biologic dose response modifiers have been added in combination therapy protocols (6,7). Furthermore, the availability of new chemotherapeutic agents such as cis-platin and taxol and

Correspondence to: Joel S. Greenberger, MD, Professor and Chairman, Department of Radiation Oncology, University of Pittsburgh Cancer Institute, 200 Lothrop Street, Rm. B336, Pittsburgh, PA 15213, U.S.A. Tel: +14126473605, greenbergerjs@upmc.edu.

biological response modifiers including bortizimab, and epidermal growth factor receptor antagonist such as C225 (cetuximab) can increase the local controllability of tumors, but also increases normal tissue toxicity (6–12). Nucleosome-targeted drugs such as bortezimab have shown effect in combined modality trials and adding this agent to C225 and chemotherapy agents supplemented with radiotherapy is undergoing a clinical investigation (7).

Squamous cell carcinomas of the head and neck region containing hypoxic areas have been shown to be susceptible to the action of hypoxic cell cytotoxins such as tirapazamine (TPZ) (13–20). The addition of TPZ to radiotherapy in protocols for the treatment of squamous cell carcinomas of the head and neck region and the lung, has shown improved local control with limited increase in toxicity (15). The addition of TPZ to combined modality chemoradiotherapy protocols of lung or head and neck cancer has shown further increases in local controllability (20).

Parallel to developments in combined modality therapy for local tumor control has been the development of agents for amelioration of the toxicity to normal tissues surrounding tumors of the head and neck region (21–30). Clinical trials have tested pentoxyphilline (26), amifostine (WR2125) (21,27,28), keratinocyte growth factor (KGF) (23), and other protective cytokines (30). These radioprotective strategies have shown some increase in therapeutic ratio and in recent studies radioprotection of normal tissue has been cited in protocols of combined modality therapy for enhanced tumor reduction.

We have developed a technique of intraoral administration of plasmid liposomes for the genes for the antioxidant enzyme manganese superoxide dismutase (MnSOD-PL) for the protection of normal tissues (31–37). In recent experiments in mice bearing orthotopic squamous cell carcinomas treated with single-dose or fractionated radiotherapy, improved local control and survival was shown by the addition of intraoral MnSOD-PL (36,38,39). The anticipated problem of simultaneous radioprotection of the tumor, abrogating the therapeutic efficacy, was not seen in recent studies demonstrating paradoxical radiosensitization of squamous cell tumors by MnSOD-PL overexpression (32,37,39). Redox balance (between squamous cell tumors and normal tissues) has been shown to explain the radioprotection by MnSOD-PL of normal oral cavity mucosa with simultaneous tumor radiosensitization (39).

In the present studies, the effectiveness of MnSOD-PL radioprotective gene therapy, combined with three tumorocidal agents (ionizing irradiation, C225, and the hypoxic cell cytotoxin, TPZ) was tested in a protocol utilizing CAL-33 human oral cavity squamous cell carcinomas, placed orthotopically in the cheeks of *nu/nu* mice.

Materials and Methods

Adult athymic nude nu animals and animal care

Athymic nude *nu/nu* mice (5 to 6 weeks of age) were obtained from Harlan Sprague Dawley, Indianapolis, USA and housed five per cage and fed standard laboratory chow. All animal protocols were approved by the University of Pittsburgh Institutional Animal Use and Care Committee (IACUC). Veterinary care was provided by the Division of Laboratory Animal Research of the University of Pittsburgh. All the protocols were supervised by the Division of Laboratory Animal Research of the University of Pittsburgh.

Cell lines

The CAL33 human squamous cell carcinoma was developed by Gioanni J. Fischel from a human oral squamous cell carcinoma of the floor of the mouth as been published previously (10). The cells were obtained from Dr. Jennifer Grandis at the Department of Otolaryngology, University of Pittsburgh School of Medicine. Cells were passaged in Dulbecco's modified

Eagle's medium in 10% fetal calf serum, supplemented with penicillin, and streptomycin and maintained in a high humidity incubator at 37°C.

MnSOD-plasmid liposomes

The pNGVL3 MnSOD-plasmid liposome complex has been described previously (36). The animals were injected intraorally with100 μl of water followed by 100 μl of MnSOD-PL containing 100 μg of plasmid DNA. In some experiments, a blank pNGVL3 plasmid minus the MnSOD transgene was used as a control plasmid.

Drugs and administration

C225 (Cetuximab) was administered intraperitoneally at 10 mg/kg in 100 μl. TPZ was provided as a white powder from William Wilson and dissolved in 50% ethanol/acetone, and then brought to 10 micromolar concentration in phosphate-buffered saline (13). TPZ was administered intraperitoneally by injection according to several protocols (13,14,20).

Animal irradiation and radiation survival curves

The mice received 14 or 18 Gy irradiation to the head and neck region using a Varian linear accelerator using 6 MeV photons with a dose rate of 300 monitor units/min (Varian Medical Systems, Inc., Palo Alto, CA, USA). The body was shielded by a 101/2 value layer bock so only the head and neck region was irradiated. The mice received single fraction irradiation according to published methods (39).

CAL-33 cell radiation survival curves were carried out *in vitro* by irradiating the CAL-33 cells in conical centrifuge tubes at 1×10^5 cells/ml of media using a J. L. Shepherd Cesium Irradiator (J. L. Shepherd and Associates, San Fernando, CA, USA) at doses ranging from 0 to 8 Gy and plating them at varying densities from 5×10^2 –5×10^4 cells per plate. Colonies of greater than 50 cells were scored at day 7. Single-hit, multi-target and linear quadratic analysis of data was calculated according to published methods (35). Parallel experiments were carried out with TPZ in normoxic and low oxygen tension (using a 3% low oxygen incubator) simulating hypoxic conditions *in vivo*. In addition, cultures of CAL-33 cells transfected with MnSOD-PL were treated with C225 (10 μM), maintained overnight under hypoxic conditions and irradiated.

Measurement of nitric oxide production following irradiation

CAL-33 cells were trypsinized, washed in media, resuspended at 1×10^6 cells per ml in Ringer's solution containing (in mmol/l) 140 NaCl, 5.2 KCl, 1.2 $MgSO_4$ 1 $CaCl_2$, 10 NaH_2PO_4/ $NaHPO_4$ and 10 glucose at pH 7.4 and irradiated at either 0 or 5 Gy. Immediately after irradiation, the tip of a porphyrinic microsensor which specifically measures NO production was placed into the cell suspension (40).

Micro-PET scanning

Animals with orthotopic tumors of 0.5 cm in diameter in the right cheek, or in some instances both cheeks, were scanned first for fluoro-meisonidaziole (FMISO) followed 48 hours later with a second scan for fluorodeoxyglucose (FDG). FMISO imaging of hypoxic centers in the tumors and FDG scanning for the detection of metabolically active areas in the tumors were carried out according to published methods (41), the latter 24 hours after FMISO scanning. Fusion scans were photographed according to published methods and injection of metabolic indicator carried out using a standard protocol (41). Each mouse was injected with 130–200 mCi of either tracer compound *via* the lateral tail vein and placed in the scanner in pairs. The animals were initially anesthetized by induction with isofluorane (5%) and maintained on 0.5–1.5% isofluorane in a 60%/40% mixture of medical air/oxygen administered by nose cone.

Body temperature was maintained throughout the experiment with a thermoelectric heating cell. Following injection, a 90-minute dynamic microPET acquisition was performed. The PET emission data were reconstructed using 2-D filtered back projection with a ramp filter. Volumes of interest (VOI) were defined over 3–4 contiguous planes for each tumor. Standardized uptake valve (SUV) was determined using the formula: SUV=(VOI activity × body mass)/injected dose. In some experiments, mice bearing CAL-33 orthotopic tumors were administered MnSOD-PL, C225, or TPZ as described above and irradiated with either 14 or 18 Gy to the orthotopic tumor 24 hours later. Twenty-four hours later the mice were injected with FMISO and scanned. The mice were injected 24 h later with FDG and scanned as described above.

Histopathology

Orthotopic CAL-33 tumors were removed 10 days after injection of 1×10^6 CAL-33 cells into the cheek of a mouse, freezing the tumor at optimum cutting temperature (OCT), sectioning it and staining the sections with hematoxylin and eosin (H&E) as previously described (31).

Combination treatment of MnSOD-PL, C225, and TPZ with irradiation

Mice of 6 weeks of age were injected with 1×10^6 CAL-33 cells into the right cheek. When the tumors became palpable (10 days after injection), the tumor size was measured using calipers and tumor volume determined using the equation volume = (length × width^2) × ½. The mice were divided into the following groups of 10: i) control, ii) 14 or 18 Gy only, iii) MnSOD-PL followed by 14 or 18 Gy 24 hours later, iv) TPZ + 14 or 18 Gy, v) C225 *i.p.* + 14 or 18 Gy, vi) MnSOD-PL + TPZ + 14 or 18 Gy, vii) MnSOD-PL + C225 + 14 or 18 Gy, viii) TPZ + C225 + 14 or 18 Gy, or ix) MnSOD-PL + TPZ + C225 + 14 or 18 Gy. The mice were injected with MnSOD-PL 24 hours before irradiation and with C225 and TPZ 10 min before irradiation. The mice were anesthetized using nembutal before irradiation to the orthotopic tumor. The tumor size was measured every 48 hours after irradiation. Once the tumors reached a size of 3 mm^3, the mice were euthanized.

Results

Radiosensitization of CAL-33 cells by MnSOD-PL transgene expression

The effect of MnSOD-PL overexpression in the CAL-33 cells was first tested with respect to radiosensitization. As shown in Figure 1, the radiation survival curve of the CAL-33 cells gave a D_0 of 1.75±0.02 Gy and ñ of 2.70±0.2. Following transfection with MnSOD-PL, significant radiosensitization was demonstrated with D_0 of 1.17±0.08 Gy (p=0.0018) and ñ of 3.50±0.5. The CAL-33 cells showed a significant increase in irradiation-induced oxidative stress as measured by nitric oxide production (Figure 2).

Effect of TPZ on tumor radiosensitization

We next evaluated the effect of TPZ on the radiosensitivity of CAL-33 cells under normoxic as well as hypoxic conditions (Figure 3). Under normal oxygen conditions, CAL-33-MnSOD cells were more sensitive to irradiation with D_0 of 1.17±0.07 Gy compared to D_0 of 1.50±0.04 Gy for hypoxia (p=0.05). TPZ resulted in no detectable killing of CAL-33-MnSOD or CAL-33 cells under normal oxygen conditions.

Cells irradiated and maintained under hypoxic conditions showed a modest increase in irradiation resistance, as would be expected from the low oxygen tension and confirming the oxygen effect (Figure 3). However, at 3% oxygen, TPZ reduced survival of both CAL-33 cells and CAL-33-MnSOD cells. Thus, expression of MnSOD did not reduce TPZ killing of CAL-33 cells during hypoxia. There was no radiosensitizing effect by adding C225 (D_0=1.58±0.09 Gy

for CAL-33-MnSOD + C225 compared to 1.61±0.09 Gy for CAL-33 + C225, respectively) *in vitro* on radiation sensitivity under hypoxia (p=0.307).

Histopathology and micro-PET scanning of CAL-33 orthotopic tumors

The histopathology of explanted CAL-33 orthotopic tumors showed blood vessel invasion (Figure 4). As shown in Figure 5, FDG and FMISO were both incorporated into the murine tumors, albeit in different regions and the 0.5 cm tumors demonstrated a central hypoxic area by FMISO staining (right side). Staining the next day with FDG showed overall metabolic hyperactivity with a less detectable area of hypoxia. PET imaging demonstrated differential uptake of [^{18}F]-FDG as compared to [^{18}F]-FMISO within CAL-33 tumors. Increased [^{18}F]-FDG uptake was noted in the anterior portion of the tumor, while [^{18}F]-FMISO uptake was increased in the posterior portion of the tumor in this mouse.

Tumor response to combined modality therapy

MnSOD-PL improved the tumor response to irradiation as shown by micro-PET scan (Figure 6). Panel A demonstrates a decrease in tumor size in MnSOD-PL and radiation-treated mice compared to those treated with radiation alone. Mice receiving irradiation and combinations of two agents or three agents are also shown in Figure 7. The effectiveness of TPZ in reducing tumor cell size alone (mouse 2) or in combination with irradiation (mouse 3) is demonstrated. The mice with orthotopic tumors receiving irradiation and all three agents (MnSOD-PL, TPZ, C225) demonstrated the overall greatest reduction in tumor cell size. These results established the effectiveness of using micro-PET scanning to assess potential additive or synergistic interactions between biological response modifiers with radiation of orthotopic tumors of the oral cavity.

Mice bearing CAL-33 in the right cheek were treated with combinations of MnSOD-PL, C225, TPZ and either 14 or 18 Gy. Tumors were measured every two days and once they reached a size of 3 mm^3 the mice were sacrificed at that time point according to IACUC protocols. A statistically significant decrease in the growth of tumor after irradiation was shown on day 10 for 14 Gy (Figure 8A) and day 8 for 18 Gy (Figure 8B) irradiation compared to nonirradiated mice (p=0.0009 or 0.004, respectively) and a significant additional reduction in tumor growth by TPZ, C225, and MC-MnSOD-PL administration compared to irradiation only at day 10 for 14 Gy (p=0.015), and day 8 for 18 Gy (p=0.0385). Other groups of animals receiving TPZ, C225, or MC-MnSOD-PL each alone, but no irradiation showed no statistically significant decrease in tumor growth compared to unirradiated controls (data not shown). The effect of 14 or 18 Gy irradiation plus one or two agents was not as effective as three agents (data not shown).

Discussion

Overexpression of MnSOD in cancer cells has been demonstrated to sensitize them to radiation, while overexpression in normal tissues protects the cells from irradiation (32,39,42). Similar results were found with the CAL-33 cells overexpressing MnSOD which were more sensitive to irradiation as seen by a decrease in D_0. These results confirmed and extended previous studies with other human and mouse squamous cell carcinoma lines derived from the oral cavity SCCVII, OC19 and Lewis lung carcinoma (42). Prior studies demonstrated increased killing of human OC19 carcinoma cells by C225 (42).

The simultaneous use of combined modality tumor treatment programs with radioprotective agents for preserving normal tissue function has gained increased importance in recent years. We have developed a technique of organ-specific administration of the antioxidant enzyme transgene (MnSOD-PL) and have shown effectiveness in models of radiation toxicity to the

oral cavity (1–2) and salivary glands (3). We demonstrated that orthotopic CAL-33 human squamous cell carcinomas in the cheek pouch of *nu/nu* mice have hypoxic centers, that these can be imaged by Micro-PET scanning, and that following administration of combinations of biological response modifiers with irradiation, tumor volume decreases, hypoxic areas are removed, and metabolically active FDG uptake-enhancing areas are also decreased. Local control as seen by a decrease in tumor growth was observed following addition of MnSOD-PL to a protocol utilizing C225, TPZ, and ionizing irradiation.

[^{18}F]-FDG PET imaging is clinically valuable in detecting areas of elevated cellular metabolism indicative of metastatic or recurrent squamous cell head and neck tumors (SCCHN) (42). To explore the role of [^{18}F]-FMISO-PET in SCCHN, we compared [^{18}F]-FDG and [^{18}F]-FMISO microPET imaging in CAL-33 tumors in *nu/nu* mice. CAL-33 cells were injected into the cheek of *nu/nu* mice (25–30 g) aged 5–6 weeks (Harlan Laboratories, Indianapolis, IN, USA) (42). Ten days later, FMISO scans demonstrated increased ^{18}F uptake in the orthotopic tumors which correlated with areas of decreased metabolic activity following FDG imaging. Combining these two imaging modalities allowed us to demonstrate hypoxic areas in the CAL-33 orthotopic tumors.

The present study uses single fractionated irradiation and single administration of the biological response modifiers. In previous studies, fractionated irradiation protocols have shown the effectiveness of multiple administrations of MnSOD-PL for radioprotection (34), and similar studies are planned for tests of the combined modality program using a new non-inflammatory mini circle plasmid MnSOD-PL (43).

The present results establish the potential effectiveness of using a normal tissue radioprotector in the setting of combined modality therapy enhancement of radiotherapeutic local control of orthotopic tumors in the head and neck region. Further studies are required to optimize methods of administration and effectiveness of these agents in a combined modality treatment of tumors of the head and neck region.

Acknowledgments

Supported by NIH Grants RO1-CA83876 and CA101837.

References

1. Agarwala SS, Cano E, Heron DE, Johnson J, Myers E, Sandulache V, Bahri S, Ferris R, Wang Y, Argiris A. Long-term outcomes with concurrent carboplatin, paclitaxel and radiation therapy for locally advanced, inoperable head and neck cancer. Annals of Oncology 2007;18:1224–1229. [PubMed: 17675395]
2. Le QT, Taira A, Budenz S, et al. Mature results from a randomized phase II trial of cisplatin plus 5-fluorouracil and radiotherapy with or without tirapazamine in patients with resectable stage IV head and neck squamous cell carcinomas. Cancer 2006;106:1940–1949. [PubMed: 16532436]
3. Kam MKM, Leung S-F, Zee B, Chau RMC, Suen JJS, Mo F, Lai M, Ho R, Cheung K-Y, Yu BKH, Chiu SKW, Choi PHK, Teo PML, Kwan W-H, Chan ATC. Prospective randomized study of intensity-modulated radiotherapy on salivary gland function in early-stage nasopharyngeal carcinoma patients. J Clin Oncol 2007;25(31):4873–4879. [PubMed: 17971582]
4. Eisbruch A. Reducing xerostomia by IMRT: What may, and may not, be achieved. J Clin Oncol 2007;25 (31):4863–4864. [PubMed: 17971579]
5. Yao M, Karnell LH, Funk GF, Lu H, Dornfeld K, Buatti JM. Health-related quality-of-life outcomes following IMRT *versus* conventional radiotherapy for oropharyngeal squamous cell carcinoma. Int J Rad Oncol Biol Phys 2007;69(5):1354–1360.

6. Thariat J, Milas L, Ang KK. Integrating radiotherapy with epidermal growth factor receptor antagonists and other molecular therapeutics for the treatment of head and neck cancer. Int J Radiat Oncol Biol Phys 2007;69(4):974–984. [PubMed: 17967298]
7. Bonner JA, Harari PM, Giralt J, et al. Radiotherapy plus cetuximab for squamous-cell carcinoma of the head and neck. N Engl J Med 2006;354(6):567–578. [PubMed: 16467544]
8. Irmer D, Funk JO, Blaukat A. EGFR kinase domain mutations – functional impact and relevance for lung cancer therapy. Oncogene 2007;26:5693–5701. [PubMed: 17353898]
9. Dent P, Reardon DB, Park JS, Bower G, Logsdon C, Valerie K, Schmidt-Ullrich R. Radiation-induced release of transforming growth factor α activates the epidermal growth factor receptor and mitogen-activated protein kinase pathway in carcinoma cells, leading to increased proliferation and protection from radiation-induced cell death. Mol Biol Cell 1999;10:2493–2506. [PubMed: 10436007]
10. Fischel J-L, Formento P, Milano G. Epidermal growth factor receptor double targeting by a tyrosine kinase inhibitor (Iressa) and a monoclonal antibody (Cetuximab) impact on cell growth and molecular factors. Br J Cancer 2005;92:1063–1068. [PubMed: 15756277]
11. Shibuya K, Komaki R, Shintani T, Itasaka S, Anderson R, Jurgensmeier JM, Milas L, Ang K, Herbst RS, O'Reilly MS. Targeted therapy against VEGFR and EGFR with ZD6474 enhances the therapeutic efficacy of irradiation in an orthotopic model of human non-small cell lung cancer. Int J Radiat Oncol Biol Phys 2007;69(5):1534–1543. [PubMed: 17889445]
12. Roeb W, Boyer A, Cavenee WK, Arden KC. PAX3-FOX01 controls expression of the $p57^{Kip2}$ cell-cycle regulator through degradation of EGFR1. Proc Nat Acad Sci USA 2007;104(46):18085–18090. [PubMed: 17986608]
13. Brown JM, Wilson WR. Exploiting tumour hypoxia in cancer treatment. Nat Rev Cancer 2004;4:437–447. [PubMed: 15170446]
14. Hicks KO, Myint H, Patterson AV, Pruijn FB, Siim BG, Patel K, Wilson WR. Oxygen dependence and extravascular transport of hypoxia-activated prodrugs: comparison of the dinitrobenzamide mustard PR-104A and tirapazamine. Int J Radiation Oncology Biol Phys 2007;69(2):560–571.
15. Rischin D, Peters I, Hicks R, et al. Phase I trial of concurrent tirapazamine, cisplatin, and radiotherapy in patients with advanced head and neck cancer. J Clin Oncol 2001;19:535–542. [PubMed: 11208848]
16. Zagorevskii D, Song M, Breneman C, et al. A mass spectrometry study of tirapazamine and its metabolites: insights into the mechanism of metabolic transformations and the characterization of reaction intermediates. J Am Soc Mass Spectrom 2003;14:881–892. [PubMed: 12892912]
17. Anderson RF, Shinde SS, Hay MP, Gamage SA, Denny WA. Activation of 3-amino-1, 2, 4-benzotriazine 1, 4-dioxide antitumor agents to oxidizing species following their one-electron reduction. J Am Chem Soc 2003;125:748–756. [PubMed: 12526674]
18. Palmer LA, Doctor A, Chhabra P, Sheram ML, Laubach VE, Karlinsey MZ, Forbes MS, Macdonald T, Gaston B. *S*-Nitrosothiols signal hypoxia-mimetic vascular pathology. J Clin Invest 2007;117(9): 2592–2600. [PubMed: 17786245]
19. Rischin D, Peters L, Fisher R, et al. Tirapazamine, cisplatin, and radiation *versus* fluorouracil, cisplatin, and radiation in patients with locally advanced head and neck cancer: a randomized phase II trial of the Trans-Tasman Radiation Oncology Group (TROG 98.02). J Clin Oncol 2005;23:79–87. [PubMed: 15625362]
20. von Pawel J, von Roemeling R, Gatzemeier U, et al. Tirapazamine plus cisplatin in advanced non-small-cell lung cancer: a report of the international CATAPULT I study group. J Clin Oncol 2000;18:1351–1359. [PubMed: 10715308]
21. Law A, Kennedy T, Pellitteri P, Wood C, Christie D, Yumen O. Efficacy and safety of subcutaneous amifostine in minimizing radiation-induced toxicities in patients receiving combined-modality treatment for squamous cell carcinoma of the head and neck. Int J Radiat Oncol Biol Phys 2007;69 (5):1361–1368. [PubMed: 17869022]
22. Chambers MS, Jones CU, Biel MA, Weber RS, Hodge KM, Chen Y, Holland JM, Ship JA, Vitti R, Armstrong I, Garden AS, Haddad R. Open-label, long-term safety study of cevimeline in the treatment of post irradiation xerostomia. Int J Radiat Oncol Biol Phys 2007;69(5):1369–1376. [PubMed: 17855005]
23. Jeschke MG, Richter G, Hofstadter F, Herndon DN, Perez-Polo J-R, Jauch K-W. Non-viral liposomal keratinocyte growth factor (KGF) cDNA gene transfer improves dermal and epidermal regeneration

through stimulation of epithelial and mesenchymal factors. Gene Ther 2002;9:1065–1074. [PubMed: 12140734]

24. Phillips TL, Kane L, Utley JF. Radioprotection of tumor and normal tissues by thiophosphate compounds. Cancer 1973;32:528–535. [PubMed: 4199352]
25. Newton GL, Aguilera JA, Kim T, Ward JF, Fahey RC. Transport of aminothiol radioprotectors into mammalian cells: passive diffusion *versus* mediated uptake. Radiat Res 1996;146:206–215. [PubMed: 8693070]
26. Rube CE, Wilfert F, Uthe D, Schmid KW, Knoop R, Willich N, Schuck A, Rube C. Modulation of radiation-induced tumour necrosis factor α (TNF-α) expression in the lung tissue by pentoxifylline. Radiother Oncol 2002;64:177–187. [PubMed: 12242128]
27. Werner-Wasik M, Axelrod RS, Friedland DP, Hauck W, Rose LJ, Chapman AE, Grubbs S, DeShields M, Curran WJ. Preliminary report on reduction of esophagitis by amifostine in patients with non-small cell lung cancer treated with chemoradiotherapy. Clin Lung Cancer 2001;2(4):284–289. [PubMed: 14720361]
28. Wasserman TH, Brizel DM. The role of amifostine as a radioprotector. Oncology 2001;15(10):1349–1354. [PubMed: 11702962]
29. Tretter L, Ronai E, Szabados G, Hermann R, Ando A, Horvath I. The effect of the radioprotector WR-2721 and WR-1065 on mitochondrial lipid peroxidation. Int J Radiat Biol 1990;57:467–478. [PubMed: 1968940]
30. Wong GHW. Protective roles of cytokines against radiation: Induction of mitochondrial MnSOD. Biochim Biophys Acta 1995;1271:205–209. [PubMed: 7599209]
31. Stickle RL, Epperly MW, Klein E, Bray JA, Greenberger JS. Prevention of irradiation-induced esophagitis by plasmid/liposome delivery of the human manganese superoxide dismutase (MnSOD) transgene. Radiat Oncol Invest Clin Basic Res 1999;7(6):204–217.
32. Epperly MW, Defilippi S, Sikora C, Gretton J, Kalend K, Greenberger JS. Intratracheal injection of manganese superoxide dismutase (MnSOD) plasmid/liposomes protects normal lung but not orthotopic tumors from irradiation. Gene Ther 2000;7(12):1011–1018. [PubMed: 10871749]
33. Epperly MW, Gretton JA, Defilippi SJ, Sikora CA, Liggitt D, Koe G, Greenberger JS. Modulation of radiation-induced cytokine elevation associated with esophagitis and esophageal stricture by manganese superoxide dismutase-plasmid/liposome (SOD-PL) gene therapy. Radiat Res 2001;155:2–14. [PubMed: 11121210]
34. Epperly MW, Kagan VE, Sikora CA, Gretton JE, Defilippi SJ, Bar-Sagi D, Greenberger JS. Manganese superoxide dismutase-plasmid/liposome (MnSOD-PL) administration protects mice from esophagitis associated with fractionated irradiation. Int J Cancer (Radiat Oncol Invest) 2001;96 (4):221–233.
35. Epperly MW, Sikora C, Defilippi S, Gretton J, Zhan Q, Kufe DW, Greenberger JS. MnSOD inhibits irradiation-induced apoptosis by stabilization of the mitochondrial membrane against the effects of SAP kinases p38 and Jnk1 translocation. Radiat Res 2002;157:568–577. [PubMed: 11966323]
36. Guo HL, Seixas-Silva JA, Epperly MW, Gretton JE, Shin DM, Greenberger JS. Prevention of irradiation-induced oral cavity mucositis by plasmid/liposome delivery of the human manganese superoxide dismutase (MnSOD) transgene. Radiat Res 2003;159:361–370. [PubMed: 12600239]
37. Guo HL, Epperly MW, Bernarding M, Nie S, Gretton J, Jefferson M, Greenberger JS. Manganese superoxide dismutase-plasmid/liposome (MnSOD-PL) intratracheal gene therapy reduction of irradiation-induced inflammatory cytokines does not protect orthotopic Lewis lung carcinomas. In Vivo 2003;17:13–22. [PubMed: 12655784]
38. Epperly MW, Carpenter M, Agarwal A, Mitra P, Nie S, Greenberger JS. Intra-oral manganese superoxide dismutase plasmid/liposome radioprotective gene therapy decreases ionizing irradiation-induced murine mucosal cell cycling and apoptosis. In Vivo 2004;18:401–410. [PubMed: 15369176]
39. Epperly MW, Wegner R, Kanai AJ, Kagan V, Greenberger EE, Nie S, Greenberger JS. Irradiated murine oral cavity orthotopic tumor antioxidant pool destabilization by MnSOD-plasmid liposome gene therapy mediates tumor radiosensitization. Radiat Res 2007;267:289–297. [PubMed: 17316075]

40. Chancellor MB, Tirney S, Mattes CE, Tzeng E, Birder LA, Kanai AJ, de Groat WC, Huard J, Yoshimura N. Nitric oxide synthase gene transfer for erectile dysfunction in a rat model. BJU Int 2003;91(7):691–696. [PubMed: 12699487]

41. Rajendran J, Mankoff DA, O'Sullivan F, Peterson LM, Schwartz DL, Conrad EU, Spence AM, Muzi M, Farwell DG, Krohn KA. Hypoxia and glucose metabolism in malignant tumors: evaluation by [^{18}F] fluoromisonidazole and [^{18}F] fluorodeoxyglucose positron-emission tomography imaging. Clin Can Res 2004;10:2245–2252.

42. Epperly MW, Franicola D, Zhang X, Nie S, Greenberger JS. Effect of EGFR receptor antagonists gefitinib (Iressa) and C225 (Cetuximab) on MnSOD-Plasmid Liposome transgene radiosensitization of a murine squamous cell carcinoma cell line. In Vivo 2006;20:791–796. [PubMed: 17203769]

43. Zhang X, Epperly MW, Kay MA, Chen Z-Y, Smith T, Franicola D, Greenberger BA, Komanduri P, Greenberger JS. Radioprotection *in vitro* and *in vivo* by mini circle plasmid carrying the human manganese superoxide dismutase transgene. Hum Gene Ther 2008;19:820–826. [PubMed: 18699723]

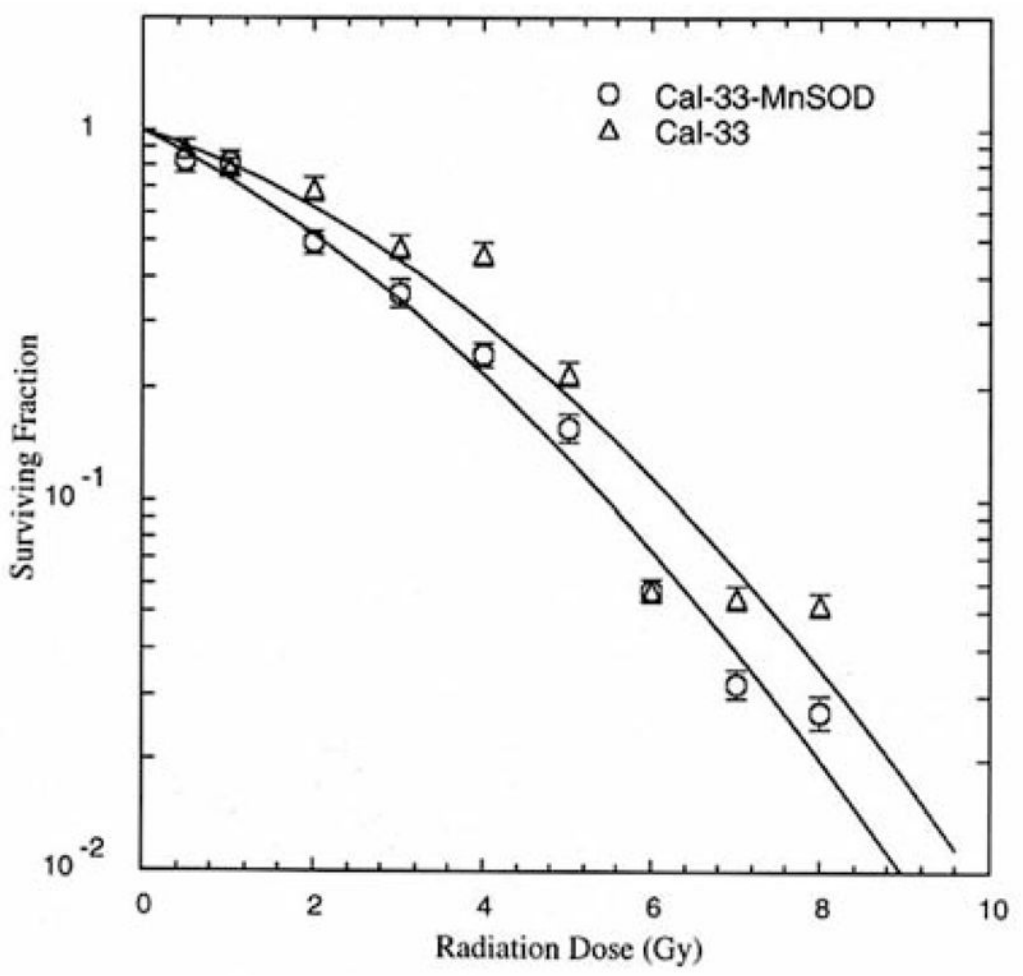

Figure 1.
Effect of MnSOD-PL transfection on radiosensitivity of CAL-33 cells. MnSOD-overexpression by MnSOD-PL transfection increases radiosensitivity by CAL-33 cells in vitro. D_0 for CAL-33 1.75±0.02 Gy, D_0 for CAL-33-MnSOD=1.17±0.08 Gy; difference is significant at p=0.0018.

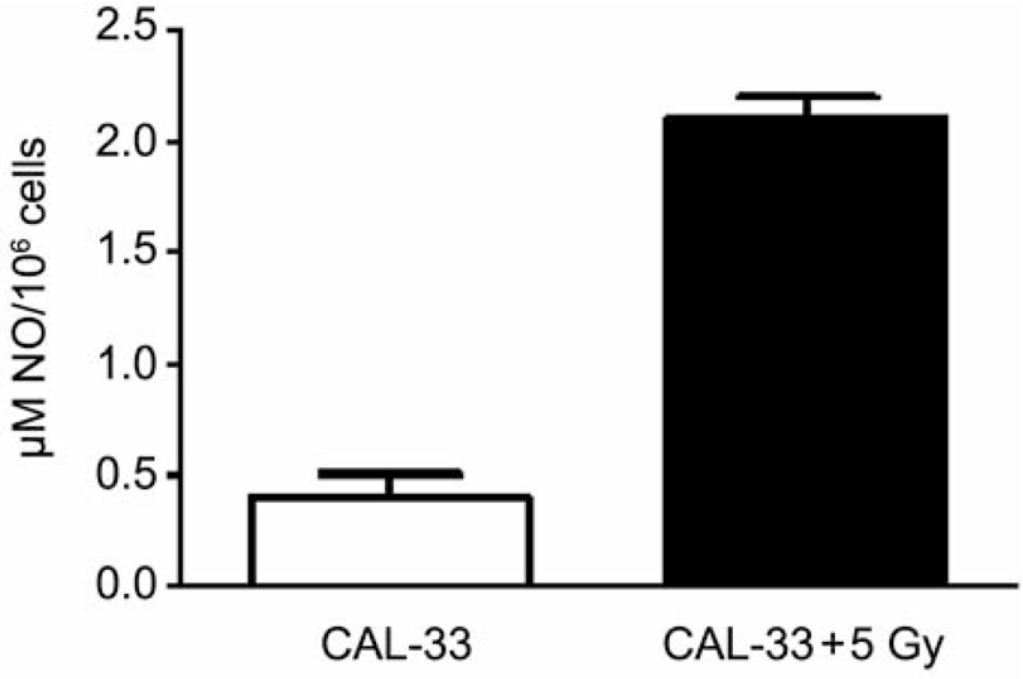

Figure 2.
Nitric oxide (NO) production measured spectrophotometrically in human CAL-33 cell pellets following irradiation.

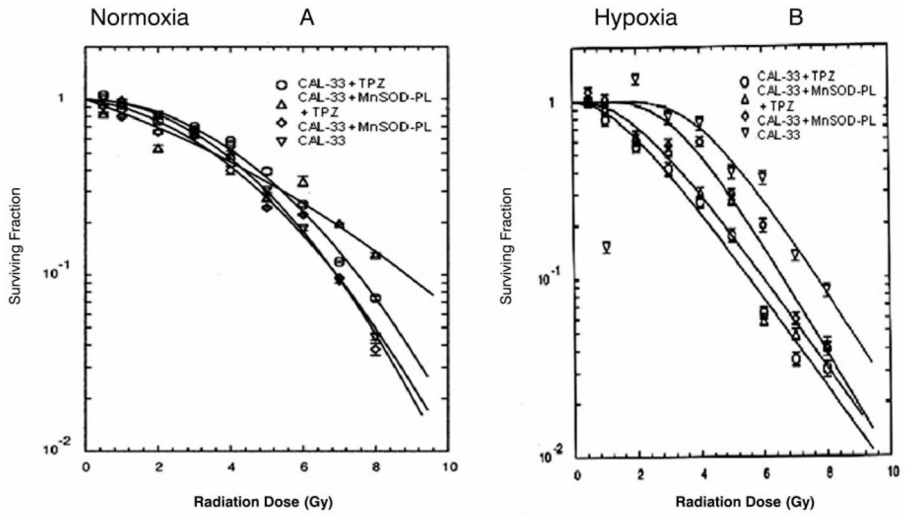

Figure 3.

Effect of TPZ on radiation killing of CAL-33 cells in vitro under normoxic (A) and hypoxic conditions (B). CAL-33 cells or MnSOD-PL transfected CAL-33 cells were either (A) incubated in TPZ 10 μM for 1 hour and irradiation survival curves performed under normal oxygen conditions, or B) held for 18 hours at 3% oxygen prior to TPZ treatment and irradiation.

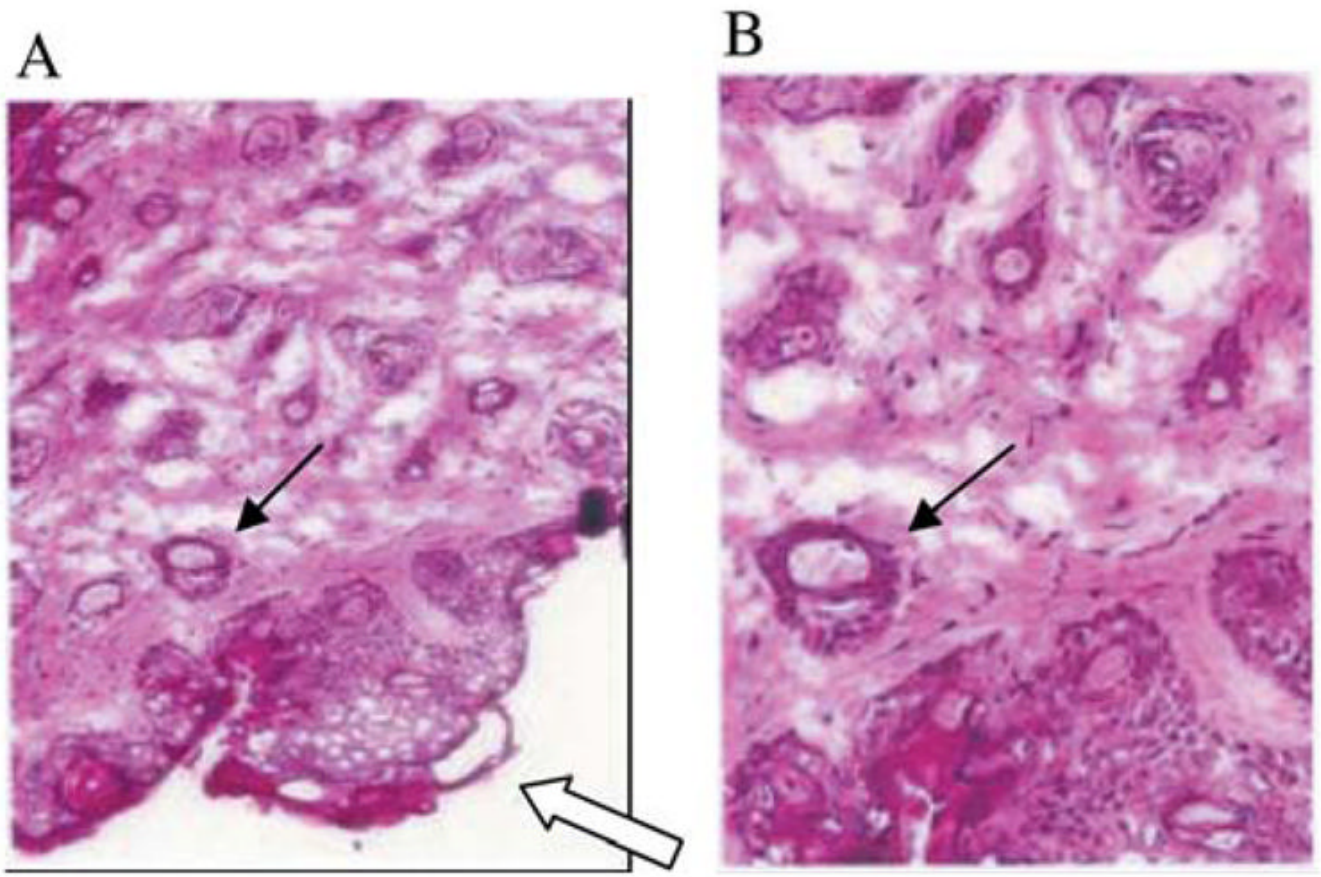

Figure 4.
Orthotopic human CAL-33 tumor in the cheek of a nu/nu mouse. Microscopic histopathology of tumor at day 10 after injection of 1×10^6 cells into the cheek (hematoxylin and eosin). Open arrow shows tumor. Closed arrow identified blood vessel, infiltration with tumor cells. A=×100, B=enlargement of A ×300.

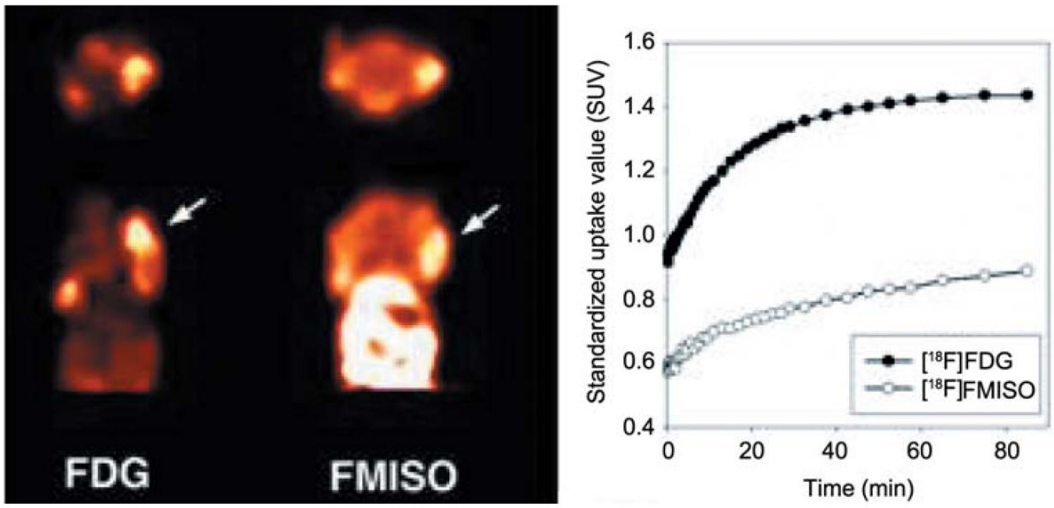

Figure 5.

PET Imaging of CAL-33 tumors in nu/nu mice ([^{18}F]-FDG vs. [^{18}F]-FMISO). Representative summed microPET images taken 40–90 min post-injection of radiotracer, with arrows indicating the location of the tumor. Representative time-activity curves of tumor uptake in mice bearing tumors following injection of [^{18}F]-FDG and [^{18}F]-FMISO. Data are expressed in terms of standardized uptake values (SUV).

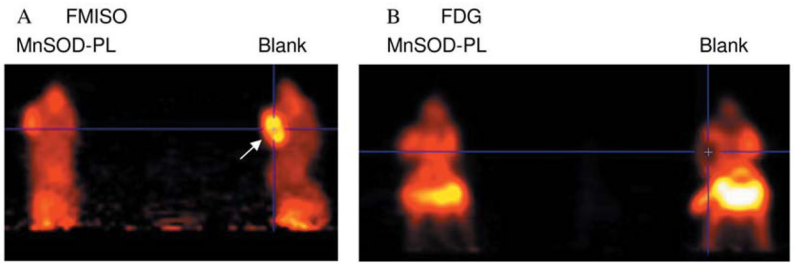

Figure 6.

Micro-PET scan showing the effect of MnSOD plus 18 Gy on CAL-33 orthotopic tumors in the cheek of athymic nude mice. Ten days after injection of 1×10^6 CAL-33 cells into each cheek, the mice were injected with MnSOD-PL 100 μg/100 μl (mouse on left) or with blank-PL (mouse on right) then irradiated with 18 Gy to the head and neck. The next day mice received i.v. FMISO (200 uCi) (A) and were scanned. Twnty-four hours later the mice were reimaged after FDG injection (B). Mouse on right in A displays a big hypoxic tumor as identified by the uptake of FMISO (yellow area – arrow); in the corresponding FDG image (B) the tumor shows reduced FDG uptake in the same region suggesting an area of necrosis or hypoxia. Mouse (left) that received MnSOD-PL shows reduced hypoxic area.

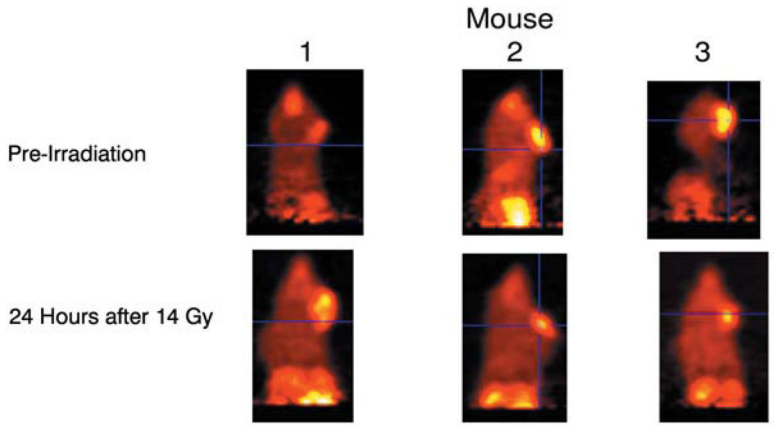

Figure 7.
Micro-PET scans showing the effect of TPZ and MnSOD-PL, plus C225, on CAL-33 orthotopic tumors in cheek of 14 Gy-irradiated nude mice. Mice were injected with FMISO before scanning. Mouse 1 is a nonirradiated control, mouse 2 was treated with TPZ (60 mg/kg) 10 min before 14 Gy, and mouse 3 with MnSOD-PL intraorally, C225, and TPZ before irradiation.

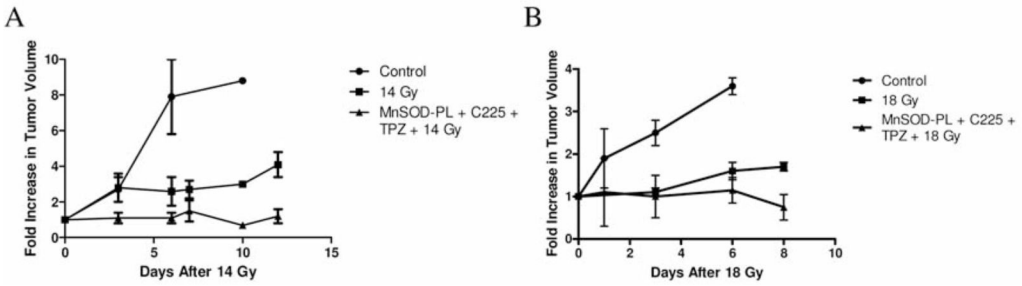

Figure 8.

Increased radiocontrollability in orthotopic oral cavity CAL-33 squamous cell carcinoma tumor-bearing nu/nu mice by tirapazamine (TPZ), cetuximab (C225), and MnSOD-PL administration. Groups of ten adult nu/nu female mice were injected in the cheek pouch with 1×10^6 CAL-33 cells. The treatments were administered at 10 days (0.3 cm diameter) and tumor volume monitored. Control: no treatment; MnSOD-PL (100 μl containing 100 μg plasmid) intraorally, TPZ (60 mg/kg) intraperitoneally in 0.1 ml, + C225 100 μl containing 10 mg/kg intraperitoneally; treated mice received either 14 Gy (A) or 18 Gy (B) to the oral cavity.